

Mineral fish: their morphological classification, usefulness as shear sense indicators and genesis

Soumyajit Mukherjee

Received: 10 October 2009 / Accepted: 20 February 2010 / Published online: 20 April 2010
© Springer-Verlag 2010

Abstract Mineral fish are sheared and commonly asymmetric mineral grains or clusters of grains. This work reports 11 sub-types of mineral fish showing a top-to-SE sense of ductile shearing in the Karakoram Metamorphic Complex (KMC). The mineral fish are of three broad geometries: sigmoid, lenticular and parallelogram. Reliable senses of shear are indicated by the overall asymmetry and inclination of mineral fish. On the other hand, the true shear sense is not always indicated by either the orientations of their cleavage planes or those of the individual grains in composite mineral fish. The ranges of local orientations of single sigmoid mineral fish that include the lower values ($<23^\circ$) in the KMC indicate their extensive ductile shearing. The studied mineral fish were products of a range of deformation mechanisms including homogeneous deformation, simple shear, intra-granular slip, crystal-plastic deformation, fracturing and synthetic shearing. Additionally, some examples might have undergone duplex slips and a few nucleated and grew either prior to or during the top-to-SE shearing.

Keywords Mineral fish · Mica Fish · Morphology · Genesis · Shear sense indicators · Ductile shearing · Karakoram

Introduction

Mineral fish are lozenge-shaped porphyroclasts and single crystals in fine-grained matrices in mylonites (Fig. 1 for micas; ten Grotenhuis 2000; ten Grotenhuis et al. 2002;

ten Grotenhuis et al. 2003; also Mukherjee and Pal 2000). Usually encountered under optical microscopes, mineral fish have commonly been used as shear sense indicators from diverse tectonic settings, viz. from a rift zone by Kula et al. (2007); from a continent–continent collision zone by Mukherjee and Koyi (2010a) and from a transform fault zone by Zhu et al. (2007). The concept of mineral fish has its origin in ‘mica fish’. These are generally asymmetric mica grains bound by micro-shear zones that are produced by crystal-plastic deformation/brittle deformation/fracturing parallel to their (001) cleavage planes/pinching at the corners (Lister and Snoke 1984). Mica fish have been considered as strain insensitive S-fabrics (Davis and Reynolds 1996). As many other sheared minerals (e.g., quartz, feldspar, chlorite, hypersthene or other pyroxenes, allanite or other epidotes, hornblende or other amphiboles, kyanite, graphite, calcite, sillimanite, leucoxene, tourmaline and pyrite) in ductile shear zones also demonstrate fish shape, the generalized term ‘mineral fish’ was coined (Mukherjee and Pal 2000; ten Grotenhuis 2000; ten Grotenhuis et al. 2003; Passchier and Trouw 2005; also see Eisbacher 1970; Lister and Snoke 1984 for the pre-existing concept).

Mica fish defined by single grains were morphologically classified into six groups: (1) lenticular, (2) lenticular with points inclined towards the foliation, (3) rhomboidal with cleavages parallel to the longest side of the fish, (4) rhomboidal with cleavages parallel to the shortest side of the fish, (5) fish with small aspect ratio and curved tails, and (6) fish with high aspect ratio and stair-stepped tails (Fig. 1; ten Grotenhuis et al. 2003). Without considering the associated tails, these morphologies can in fact be viewed under three supergroups: (a) sigmoid (covering groups 2 and 6); (b) lenticular (including groups 1 and 5); and (c) parallelogram (incorporating groups 3 and 4). On the other hand, as by-products of other studies, mineral fish

S. Mukherjee (✉)
Department of Earth Sciences, Indian Institute of Technology
Bombay, Powai, Mumbai 400 076, Maharashtra, India
e-mail: soumyajitm@gmail.com

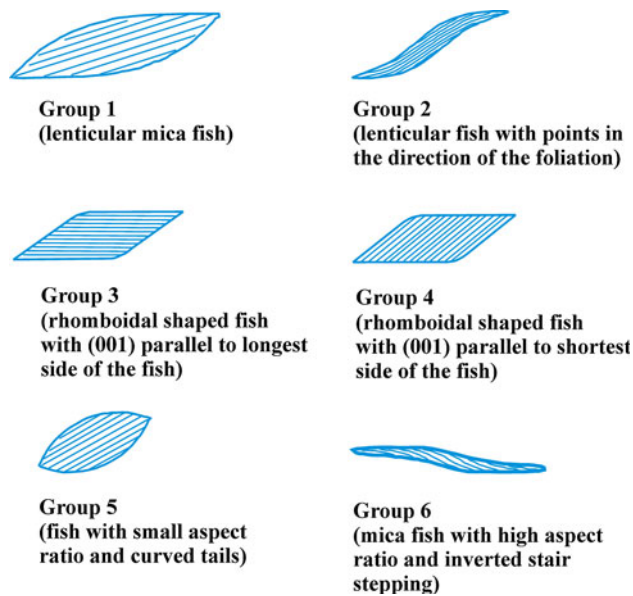


Fig. 1 Morphology of mica fish, groups 1–6, is reproduced from fig. 4 of ten Grotenhuis et al. (2003)

were also defined for mineral aggregates (e.g., Singh 2003; Stephenson 1997; Stephenson et al. 2000; Mukherjee 2007; Mukherjee and Koyi 2010b). Therefore, it will be useful to provide a new morphological classification of mineral fish that can incorporate such mineral aggregates and also any new varieties. This work aims to (i) broaden the existing morphologic classification of mineral fish by defining morphologic terms; and in addition (ii) to use microstructural observations to decipher their genesis. These studies are based on thin sections of ductile sheared rocks from the Karakoram Metamorphic Complex, India.

The study area

The Karakoram Metamorphic Complex (KMC) occurs at the southern edge of the Eurasian plate as two Paleozoic-Mesozoic metamorphic belts: (i) the Tangste Group with high-grade sillimanite-bearing garnet schists and gneisses, amphibolites, leucogranites and migmatites; and (ii) the Pangong Group with phyllites, marbles, greenschists, amphibolites and mylonites (Fig. 2). The KMC rocks underwent greenschist to amphibolite facies metamorphism, and demonstrate a main foliation that dips steeply towards NE and SW, a stretching lineation that plunges gently NW and SE and a top-to-SE sense of ductile shearing (Thakur 1992; Jain et al. 2003; fig. 7 of Jain and Singh 2008). The studied thin sections are perpendicular to the main foliation and parallel to the stretching lineation so that the ductile shear sense indicators encountered represent the true sense of regional shearing.

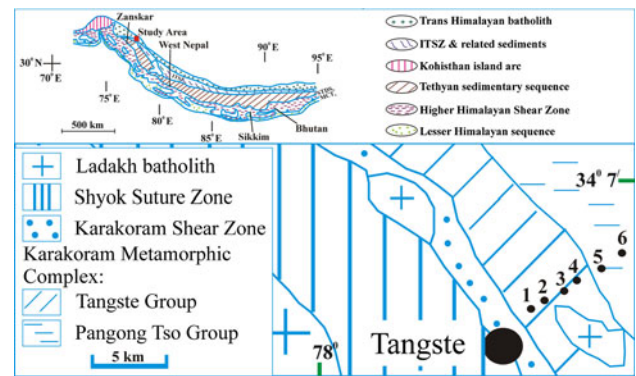


Fig. 2 Simplified geologic map of the study area and sample locations at the northern margin of the western Himalaya. The map is a partial reproduction from fig. 1 of Jain and Singh (2008). The inset map of the Himalaya is reproduced from fig. 1 of Godin et al. (2006)

Morphological classification and usefulness as shear sense indicators

Mineral fish in the KMC are defined either by a single mineral grain or by an aggregate. Hence, mineral fish are classified into the following two broad categories: (1) *single fish* and (2) *composite fish*.

(1) Single fish (Figs. 3a–d, 6a–d, 8a–d, 12d)

These occur as isolated mineral grains that may be interconnected with other single fish by a trail of recrystallized micas wrapped by micas. Depending on the geometry of the single mineral fish, they are classified as follows.

(1a) Sigmoid fish: (Fig. 3a–c, grain 2 of Fig. 3d, grains 1–3 of Fig. 6a, b)

Boundaries of such single mineral fish are sigmoid shaped. The following terms and parameters are defined on the sigmoid fish (Fig. 4a–c). The two tapering points of a mineral fish with tightest curvature are named as *tips* (Fig. 4a–c). Instead of having tip(s), some fish possess re-entrant(s) or *mouth(s)* (Fig. 4b) similar to many boudins. The line joining the tips is called the *diagonal* (*D*) (Fig. 4a). ‘*D*’ has also been referred to as the ‘long-axis’ by Simpson and Schmid (1983) and the ‘long diagonal’ by Mancktelow et al. (2002) for sheared grains in other contexts. The *maximum thickness* of the fish measured perpendicular to the diagonal (*D*) is denoted by ‘ T_{\max} ’ (Fig. 4a). The *Aspect ratio* is defined as $R = D T_{\max}^{-1}$ (Fig. 4a). The C-planes that bound mineral fish can be deciphered by either (i) the foliation defined by minerals, most often micas; or (ii) much smaller fragments of the fish that are parallel to, and hence are the same as the mylonitic foliation and are called

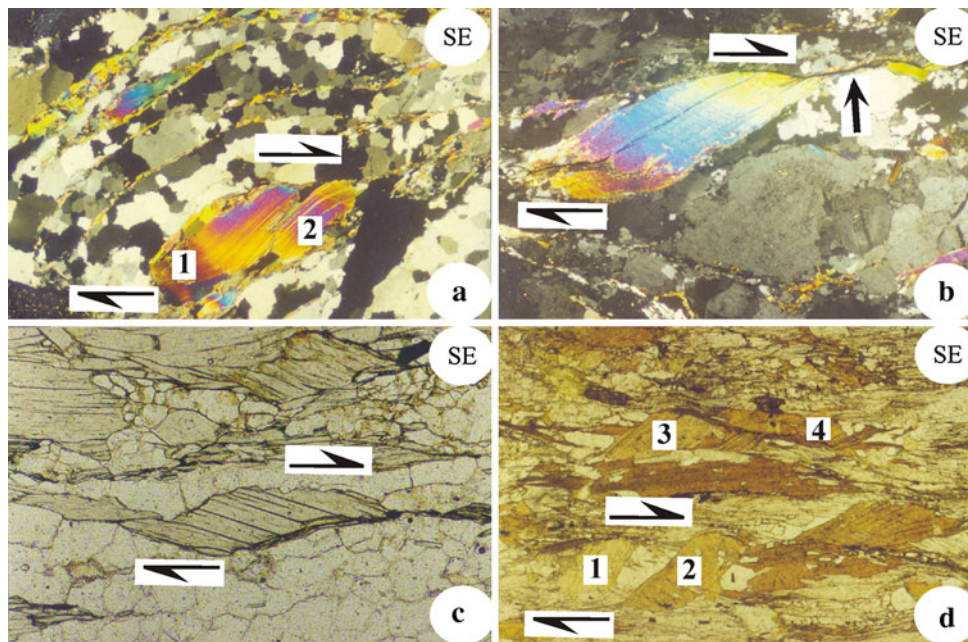


Fig. 3 Single sigmoid fish of a number of local orientations (α) define its different types. Shear sense: top-to-SE. **a** Two single steep sigmoid mica fish 1 ($\alpha = 36^\circ$, $R = 2.5$) and 2 ($\alpha = 41^\circ$, $R = 3.7$) with sigmoidally bent cleavages parallel to the fish boundaries. Dynamic recrystallization affected the entire boundaries of both the fish. Thin-section number: K3. Photo in cross polarized light. Length of the photo: 2 mm. **b** An elongated sigmoid muscovite fish ($\alpha = 20^\circ$, $R = 4.2$) with almost straight boundary. Distinct long straight fish tail (full arrow) of very fine-grained recrystallized materials defines the C-plane. Thin-section number: K5. Photo in cross polarized light. Length of the photo: 5 mm. **c** An elongated sigmoid muscovite fish ($\alpha = 18^\circ$, $R = 4.8$). Cleavage planes are at an obtuse angle to the

shear direction. Individual cleavage blocks of this fish are parallelogram shaped. The fish boundary is strongly corroded and modified systematically by pressure solution to give an overall sigmoid shape. Thin-section number: K1. Photo in plane polarized light. Length of the photo: 2 mm. **d** A top-to-SE sense of shear displayed by grain 1: r-parallel biotite fish ($\alpha = 51^\circ$, $R = 1.3$), and grain 2: a steep sigmoid biotite fish ($\alpha = 42^\circ$, $R = 3.4$). The other sheared biotite grains '3' and '4' are of irregular shape. A shearing converted '1' and '2' into fish shape, grain 1 escaped pressure solution at its corners. Grain 2 underwent pressure solution leading to smoothening of a pair of corners. Thin-section number: K6. Photo in plane polarized light. Length of the photo: 1 mm

fish trails or tails. Orienting the primary shear planes bounding the mineral fish parallel to the E-W axis of the objective, the highest point in the mineral fish boundary is denoted as its 'crest' (Fig. 4c) and the lowest point as a 'trough'. The C-planes are tangents to the mineral fish at these two points. Mineral fish unaffected by secondary shearing (or the C' and C'' shearing of Passchier and Trouw 2005) demonstrate a 'crest region' and a 'trough region' (Fig. 4a, b). These regions are short and linear traces on the mineral fish parallel to the C-planes. On rotating the stage of the microscope by 180° , the crest or the crest region interchanges with the trough or the trough region. Let 'P' be the point of intersection between the mineral fish boundary and the line representing the maximum thickness ' T_{\max} ' (Fig. 4a). The acute angle between the tangent at 'P' and the C-plane defines the local orientation (for the term refer to Blenkinsop and Treloar 1995) of the mineral fish (Fig. 4a). Note that the tangent at P need not be parallel to the diagonal for all the single sigmoid mineral fish. Two points of minimum curvature on the mineral fish boundary across the diagonal are the inflection points (I and I') (Fig. 4a). Where

the line II' intersects the diagonal (D) is the point of inversion 'O' (Fig. 4a). For an ideal sigmoid shape, any point on the fish boundary should correspond to another point on the boundary across the diagonal and equidistant from 'O'.

Sixty-nine grains of single sigmoid mineral fish with sharp tips and grain boundaries unaffected by recrystallization (so that accurate measurement of ' D ', ' T_{\max} ' and hence ' R ', and ' α ' are possible) were plotted on a graph of local orientation (α) versus aspect ratio (R). The mineral fish plot within wide ranges of local orientation (α) = 0 – 43° and aspect ratio (R) = 2 – 11.1 with a maximum concentration of 21 grains between $\alpha = 10$ – 18° and $R = 2.1$ – 10 (Fig. 5). In this plot, (i) no simple increasing or decreasing relation between ' R ' and ' α ' is noted; (ii) there exists 9 grains for which $\alpha = 10^\circ$ and R varies from 3 to 10; and (iii) natural breaks in mineral fish are noted at α around 23 and 7° . Most plausibly, these overlaps and gaps in the plots are due to unequal size and random orientation of the unshered minerals before the onset of deformation. Based on Fig. 5, the three following types of sigmoid fish are defined.

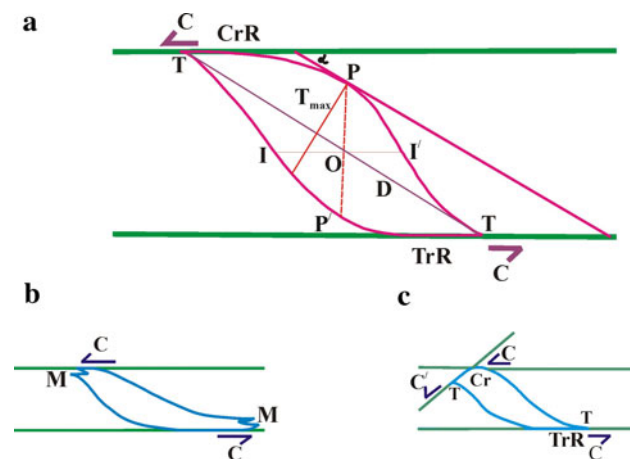


Fig. 4 Morphology of single sigmoid mineral fish. **a** is that of a fish unaffected by secondary shearing: T, tip; CR, crest region; TrR, trough region; D, diagonal; T_{max} , maximum thickness of the mineral fish measured perpendicular to D; P, point of intersection between the mineral fish boundary and the line marking T_{max} . Aspect Ratio $R = D T_{max}^{-1}$; α (local orientation), acute angle between C-plane and the tangent to the mineral fish boundary drawn at point P; I, I', inflection points; O, point of inversion, obtained by intersection between II' and D. **b** is that of a mineral fish with mouths instead of tips (not affected by secondary shearing). **c** Shows a mineral fish with one of its tips affected by secondary shearing. The crest (C) near this tip is defined as a sharp point, the trough is defined as a region (TrR), instead of a point, since the tip nearest to it has not suffered secondary shearing

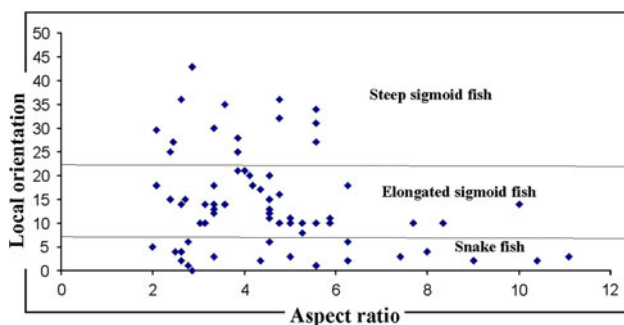


Fig. 5 Single sigmoid mineral fish with sharp tips and grain boundaries are plotted in a graph of local orientation (α) versus aspect ratio (R). Domains of steep sigmoid-, elongated sigmoid- and snake fish are shown

(1a1) *Steep sigmoid fish* (Fig. 3a, grain 2 in Figs. 3d, 6a) The lower limit of local orientation (α) of these fish is fixed as 23° with its observed upper limit in the samples being 43° . Within this limit of local orientation (α), the aspect ratio (R) ranges from 2.08 to 5.6 (14 measurements). Such mineral fish resemble ‘ σ -Type porphyroclast system’ of Simpson (1986), ‘ σ_a -Type porphyroclast system’ of Passchier and Simpson (1986), ‘porphyroclastic type’ of Blenkinsop and Treloar (1995) and group-2 mica fish of ten Grotenhuis et al. (2003). However, while the sigma structure is defined by tapering pressure shadows of other minerals at a pair of opposite corners of the

porphyroblastic minerals (as per fig. 5.27e of Passchier and Trouw 2005), the sheared mineral body alone defines the steep sigmoid fish shape.

(1a2) *Elongated sigmoid fish* (Fig. 3b; grains 1 and 3 of Figs. 6a, 12d) This is a variety of single sigmoid fish that are inclined at a lower angle with the C-shear plane. The local orientation (α) of the elongated sigmoid fish is limited between 7 and 23° where the aspect ratio (R) lies within 3.1 to 10 (35 measurements). Any one of the boundaries of these fish can have curvature less than those of the steep sigmoid fish. These fish resemble morphologically the ‘banded type’ porphyroclasts of Blenkinsop and Treloar (1995). From Fig. 5, it can be stated that elongated sigmoid fish need not always have higher aspect ratios than that of the steep sigmoid fish.

The asymmetric shapes of steep sigmoid and elongated sigmoid mineral fish give a top-to-SE sense of shear that matches with the other shear sense indicators in the thin sections. This renders them reliable guides in primary shear sense determination. The single set of cleavage planes in such fish, if present and visible, are either curved throughout and sub-parallel to the fish boundary (Fig. 3a; grain 2 in Fig. 6a) or are nearly straight with mild or strong curvatures only near the fish boundary (Fig. 3b). The cleavage planes of mica fish are usually inclined in the same direction as that of its diagonal (Figs. 3a, b, d, 6a, b, 8b, d, 12c). However, cleavages of single sigmoid mineral fish are very rarely found to be oriented antithetic to the shear sense i.e., they rarely have an acute angle with the sense of shear (Fig. 3c, also refer to fig. 6e of Little et al. 2002). Thus, the cleavage plane orientation in mineral fish alone should not be taken as reliable shear sense indicators, especially if the mineral fish had partly lost its characteristic shape by recrystallization along its boundaries. The most obvious explanation (Fig. 7) for mineral fish with cleavages antithetic to the C-planes is that the cleavages were antithetic to the C-planes also before shearing was initiated. Due to shearing, the cleavage planes reached a steeper orientation to the C-plane (stage 3 in Fig. 7) and pressure solution gave rise to the sigmoid shape at that stage. Given the possibility of heterogeneous deformation as discussed in “Genesis” in this paper, the presented model of deformation of the mica grain is certainly a simplification.

(1a3) *Snake fish* (Figs. 5, 6b) This is a single sigmoid fish with a very low local orientation ($\alpha = 0\text{--}7^\circ$) and a much wider range of aspect ratios ($R = 2.6\text{--}11.1$) (10 measurements). These fish are nearly similar to group-6 mica fish of ten Grotenhuis et al. (2003). Affected by pronounced synthetic secondary C'-shear related to top-to-SE regional primary shearing, these fish could be extremely elongated.

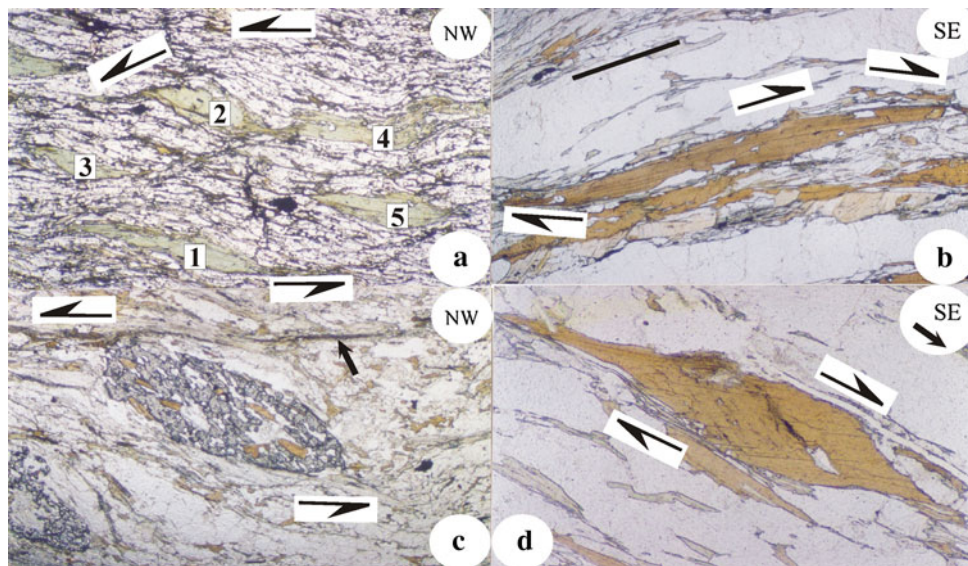


Fig. 6 Top-to-SE sheared single mineral fish of different morphologies. **a** Two elongated sigmoid- (grain 1: $\alpha = 16^\circ$, $R = 3$; grain 3: $\alpha = 13^\circ$, $R = 3.1$) and a steep sigmoid (grain 2: $\alpha = 28^\circ$, $R = 2.2$) chlorite fish. Grains 4 and 5 are of intermediate shape. The cleavage planes of grains '1' and '2' are sub-parallel to the elongated sigmoid fish boundary. Grain '2': secondary shearing affected the left tip so that the crest is defined as a point. Thin-section number: K3. Photo in plane polarized light. Length of the photo: 2 mm. **b** A snake fish of biotite ($\alpha = 3^\circ$, $R = 11.1$) with cleavage traces parallel to its boundary. The primary shear plane is shown by a black line. Synthetic shearing near the tips is prominent. Thin-section number:

K3. Photo in plane polarized light. Length of the photo: 2 mm. **c** A single lenticular garnet fish of different minerals display a top-to-SE sense. Garnet fish ($\alpha = 32^\circ$, $R = 3$) with rounded tips. The C-plane is thick and straight (full arrow). Thin-section number: K3. Photo in plane polarized light. Length of the photo: 2 mm. **d** A single lenticular biotite fish ($\alpha = 0^\circ$, $R = 5.3$) with extremely elongated tips. Inclined cleavage planes of the fish indicate the shear sense that eventually matches with the other shear sense indicators in the thin section. Thin-section number: K3. Photo in plane polarized light. Length of the photo: 2 mm

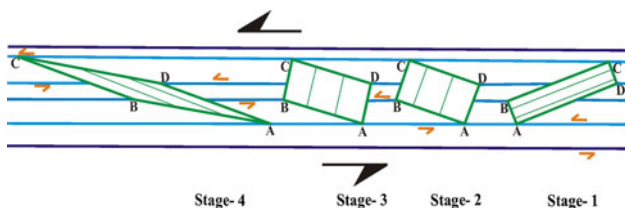


Fig. 7 Top-to-left progressive simple shear on a rectangle ABCD representing a mica grain as if drawn on a pack of cards. Cleavages of this grain are parallel to the side AD and initially (stage 1) at an acute angle to the shear direction. With progressive shear, cleavages orient steeper to the shear plane (stage 2 and 3), become perpendicular and then attain a gentle angle (stage 4). The process also involves slip along the cleavage planes. The presented model is undoubtedly a simplification

(1b) Lenticular fish (Fig. 6c, d)

These fish are elliptical in shape and are therefore similar to the augens in augen-gneisses and to group-1 and -5 mica fish of ten Grotenhuis et al. (2003). Unlike sigmoid fish (Fig. 4a), such fish lack inflection points (I, I') and were encountered with wide ranges of local orientations (α) between 0 and 35° and aspect ratios (R) between 1.35 and 6.2 (15 measurements). Both the tips (Fig. 6d) may be exceedingly elongated indicating flattening perpendicular

to (or pulling parallel to) their diagonal (D). For lenticular fish, the diagonal (D) coincides with the major axis and the ' T_{max} ' with the minor axis of the elliptic shape.

(1c) Parallelogram fish (Fig. 8a–c)

These minerals fish are shaped like parallelograms with two of their boundaries usually parallel to the C-planes. The observed local orientations (α) ranges from 30 to 46° and the aspect ratios (R) between 3.13 and 6.8 (18 measurements). This range of ' α ' is much broader than 50–55° as compiled from the parallelogram-shaped tourmaline fish documented near Lambari in Brazil (ten Grotenhuis et al. 2002). The problem in determining shear sense from parallelogram mineral fish is that their shape can be generated by ductile shearing from two rectangular grains with different orientations (Fig. 9). However, this ambiguity can be resolved after inferring the orientation of the C-plane by tracing the matrix foliation and/or the fish trail, and then interpreting the pre-shear rectangle. Using this technique, a uniform top-to-SE shear sense was deciphered from the KMC (Fig. 8a–c).

With respect to their pair of boundaries parallel to the C-planes, parallelogram mineral fish are further classified

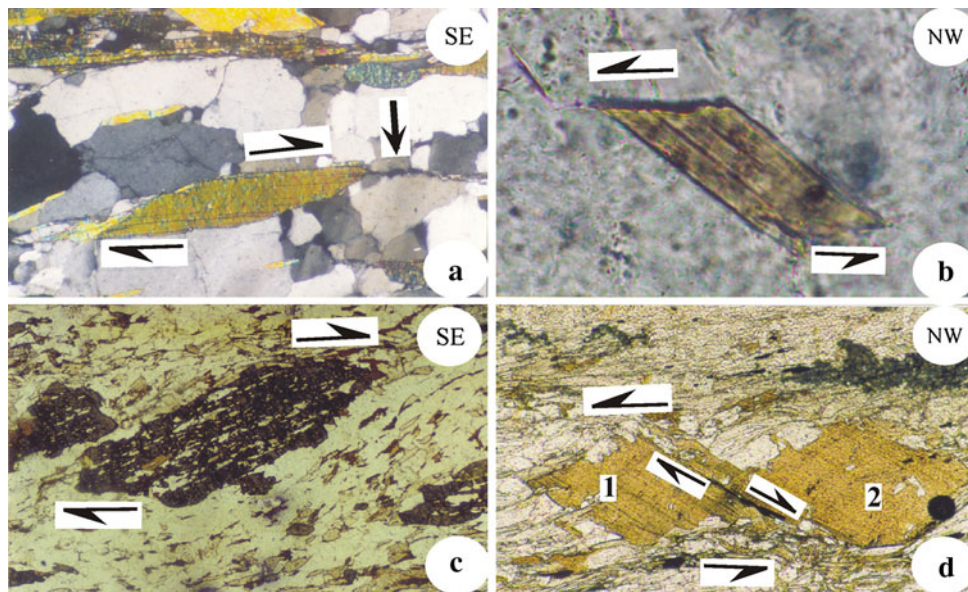


Fig. 8 Parallelogram fish of different minerals and sub-types. Top-to-SE shear sense displayed. **a** An l-parallelogram fish ($\alpha = 20^\circ$, $R = 5.3$). Long straight C-foliation occurs beside the right tip of the fish (full arrow). Thin-section number: K3. Photo in cross polarized light. Length of the photo: 1 mm. **b** An r-parallelogram muscovite fish ($\alpha = 44^\circ$; $R = 3$). The sense was deciphered after knowing the C-plane orientation outside the field of view. Thin-section number:

K3. Photo in cross polarized light. Length of the photo: 2 mm. **c** A garnet fish ($\alpha = 30^\circ$, $R = 3$) that cannot be classified into r- or l-type since it lacks cleavage. Thin-section number: K3. Photo in cross polarized light. Length of the photo: 5 mm. **d** Two r-parallelogram biotite fish (grain 1: $\alpha = 33^\circ$, $R = 2.1$; grain 2: $\alpha = 31^\circ$, $R = 1.7$) display grain to grain slip. Thin-section number: K3. Photo in cross polarized light. Length of the photo: 2 mm

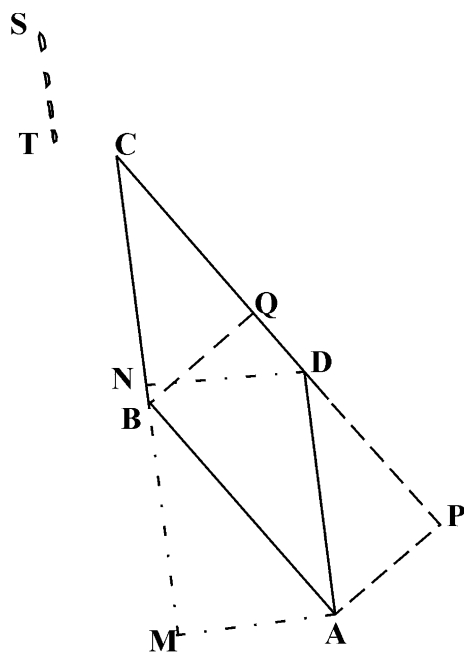


Fig. 9 Geometric representation of the fact that a single parallelogram mineral fish ABCD can be derived by simple shear on rectangular un-sheared mineral grains—AMND and APQB—of two different orientations. To find the true sense of shear, primary shear plane/main foliation in the rock matrix is to be identified. If the foliation is identified to be ST, shearing took place parallel to itself. Thus the rectangle AMDN was the orientation of the mineral grain before the onset of shearing

into the following sub-types: (1c1) *l-parallelogram fish*: these fish have their cleavage planes parallel to the C-planes (Fig. 8a) and (1c2) *r-parallelogram fish*: the cleavages of these fish are at an angle with the primary shear planes (grain 1 in Figs. 3d, 8b, d). The l-parallelogram fish resemble group-3 mica fish of ten Grotenhuis et al. (2003) and r-parallelogram fish with their group-4 fish. However, parallelogram mineral fish lacking cleavages (the garnet fish in Fig. 8c) or having more than one set of visible cleavages (such as amphibole- or calcite fish) that are visible in the thin section cannot be classified into the l- and the r- categories. At the initial un-sheared condition, the cleavage planes of the l-parallelogram fish must had been parallel and the r-parallelogram fish oblique and at a higher angle to the C-planes. Interestingly, parallelogram-shaped micas nucleated randomly over a pre-existing foliation may not at all be a product of shearing as their parallelogram shape might also arise from grain overlap (Figs. 10a, 11). Such parallelogram-shaped minerals that are not bound by any C-planes are not included in the mineral fish category. Parallelogram shape can also arise in un-sheared minerals (such as un-sheared amphiboles) in specific natural sections and thin sections. Therefore, unless a number of unambiguous shear sense indicators and decipherable mylonitic foliations are found in the same section, the parallelogram shapes alone should not be considered as ‘fish’ nor as true shear sense indicators.

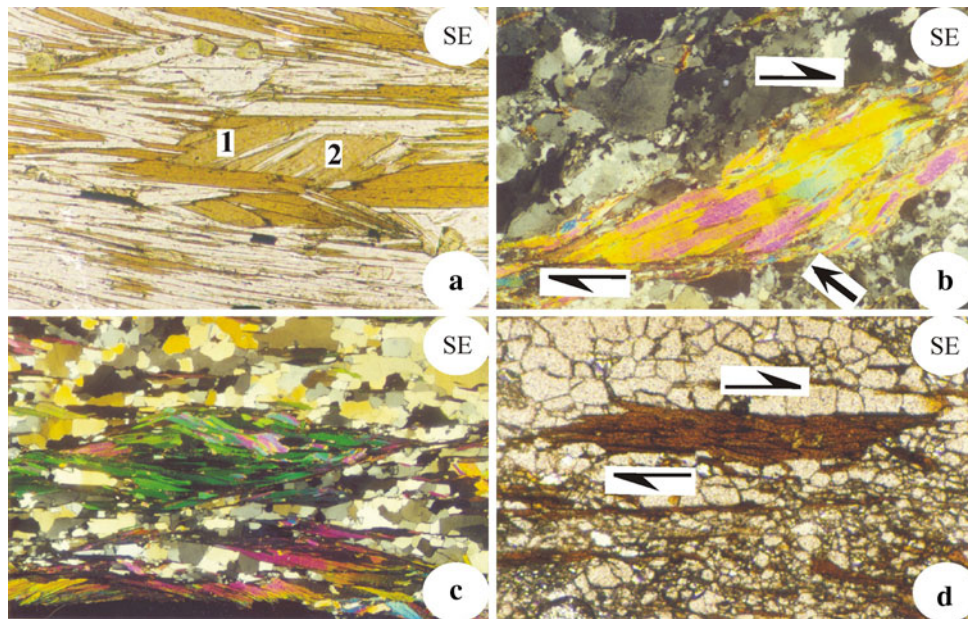


Fig. 10 **a** Few of the haphazardly grown biotite grains- '1' and '2'- on the foliation plane, are parallelogram shaped. The shape is due to overlap of the surrounding mica grains. Therefore, no attempt should be made to deduce the sense of shearing from these grains. Thin-section number: K3. Photo in plane polarized light. Length of the photo: 2 mm. **b** Sigmoid foliation fish of mica grains. Its shape asymmetry gives a top-to-SE sense of shear. The thick C-plane sharply truncates the sigmoid aggregate (*full arrow*). Thin-section number: K6. Photo in cross polarized light. Length of the photo:

2 mm. **c** Lenticular foliation fish of mica grains at very low angle to the C-plane. The constituent mica grains are variably oriented and are not indicative of the shear sense. Thin-section number: K2. Photo in cross polarized light. Length of the photo: 2 mm. **d** Parallelogram foliation fish of biotite grains showing a top-to-SE sense of shear. Individual biotite grains in the aggregate do not represent the sense of shear. Thin-section number: K5. Photo in plane polarized light. Length of the photo: 2 mm

For parallelogram fish with a pair of boundaries parallel to the C-planes (Fig. 8a–c), the followings points are noted. (1) The local orientation (α) is more easily defined as the acute angle between the C-plane and the straight fish boundary that is inclined to the C-plane. (2) The crest region and the trough region coincide with a pair of parallel boundaries of the fish that are parallel to the C-plane. Of all the different single mineral fish, only the sigmoid, elongated sigmoid and lenticular fish seldom exhibit single or double mouths instead of tip(s) (Fig. 4b). The grain boundaries of less rigid mineral fish, especially those of micas, are seldom affected by dynamic recrystallization (Fig. 3a).

(2) Composite fish (Figs. 10a–d, 12a–c)

Such fish are defined by more than one mineral grain. Composite mineral fish are subdivided into the following types.

(2a) Foliation fish (Fig. 10b–d)

The term 'foliation fish' (also called 'tectonic fish') was used by Dennis and Secor (1987), Hammer and Passchier (1991) and Davis and Reynolds (1996) as internal back-rotated packets of foliations within ellipsoidal asymmetric rock volumes inclined to the external foliation within the rock

matrix. Passchier and Trouw (2005) defined 'foliation fish' as a fish composed of layers of polycrystalline micas. Passchier and Trouw (2005), Mukherjee and Koyi (2010b) and Trouw et al. (2010) documented foliation fish of sigmoid shapes only. Recently Mukherjee (2010b) in his fig. 3b recorded lenticle-shaped foliation fish as well. In this work, the term is applied similar to the usage by Stephenson (1997), Lin (1999) and Stephenson et al. (2000) to denote ductile sheared aggregates of minerals of the same or different species (Fig. 10b–d). More rigid or stiffer quartzo-feldspathic minerals and recrystallized quartz also defines foliation fish by being wrapped by micas (such as figs. 6a,b of Mukherjee, 2010a). Depending on their overall geometries, foliation fish are classified into: (2a1) *sigmoid foliation fish* (Fig. 10b), (2a2) *lenticular foliation fish* (Fig. 10c) and (2a3) *parallelogram foliation fish* (Fig. 10d). The shear senses of sigmoid- and parallelogram foliation fish can easily be ascertained from their asymmetries. Foliations affected by bulk, inhomogeneous shortening are expected to be anastomosing (e.g., Bell 1981). Lack of anastomosing fabric in foliation fish point out that they are not products of bulk, inhomogeneous shortening (nor pure shear). Therefore, as their shape asymmetry matches with the top-to-SE sense given by the single fish, the foliation fish are presumably the products of simple shearing.

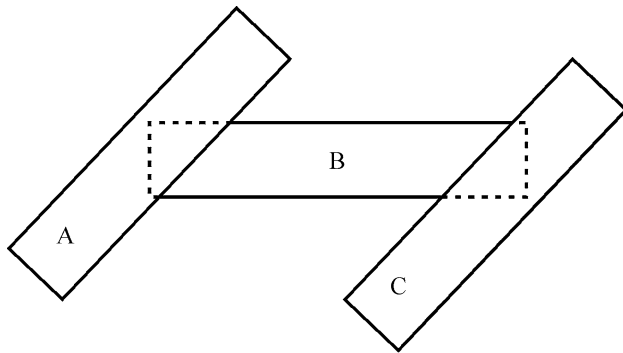


Fig. 11 Diagrammatic presentation of the fact that overlap of two rectangular mica grains 'A' and 'C' over 'B' can give rise to an apparent parallelogram shape of grain 'B'

The observed lenticular foliation fish are oriented at very low angle (similar to ' α ') to the C-planes. This renders them unfit in construing their shear sense. The inclination of the steep sigmoid-, elongated sigmoid- and the parallelogram foliation fish to the C-plane consistently shows a top-to-SE sense of shearing of the KMC. Some of the individual minerals that constitute the composite fish, however, do not match with this shear sense. For this

reason, it is suggested that none of these grains should be used in independent determination of shear sense (especially Fig. 10c, d).

(2b) *Cross-cutting fish (Fig. 12a, b)*

One mineral fish partially or completely cuts across the other to give a number of cross-cutting fish. The shapes of the individual fish are usually sigmoid and all record the same top-to-SE sense of shearing in the KMC.

(2c) *Internal fish (Fig. 12c)*

In this case, one mineral fish nucleates inside the other mineral fish and both of them display the same top-to-SE sense of shearing (also see fig. 8a of Mukherjee 2010a). Internal fish are rare, the two minerals that define this type of fish are always micas in the KMC, and the nucleated fish is visible only under a very high magnification. While the larger mica fish can be sigmoid, parallelogram or lenticular shaped, the smaller one is found to be either sigmoid or parallelogram. When the nucleated fish is parallelogram shaped, two of its boundaries are parallel to the cleavages of the host mineral fish. The internal fish, the cross-cutting

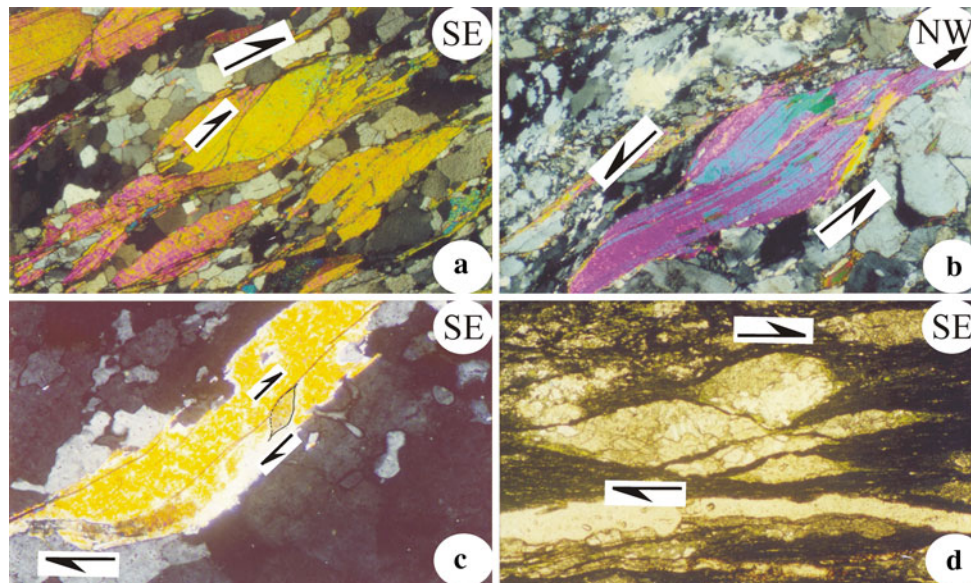


Fig. 12 **a, b** Cross-cutting mica fish display a top-to-SE shear sense. **a** Shows overriding of mica grains in a piggy-back manner over muscovite fish '1'. ' α ' of the fish '1' is 30° and R is 3. Thin-section number: K1. Photo in cross polarized light. Length of the photo: 2 mm. **b** Shows fish '1' and '2' with a low $\alpha \sim 20^\circ$. Thin-section number: K4. Photo in cross polarized light. Length of the photo: 1 mm. **c** Internal biotite fish within a large muscovite fish with a pair of boundaries of the internal fish parallel to the cleavage traces of the

later. Shape asymmetry of both the fish indicate a top-to-SE sense of shear. Thin-section number: K4. Photo in cross polarized light. Length of the photo: 1 mm. **d** An elongated sigmoid calcite fish later fractured into two grains '1' and '2'. Restoring these fragments, α of the original fish is calculated as 20° and R as 4.7. The fragment '1' resembles a parallelogram or a lenticle shape. Thin-section number: K5. Photo in plane polarized light. Length of the photo: 2 mm

fish and the three varieties of foliation fish are formal additions in the category of mineral fish.

Genesis

Based on the observed limited range of the angle 8–32° of the long-axis of mica fish with the C-planes in a Brazilian shear zone, ten Grotenhuis et al. (2003) proposed that mica fish acquire a stable state of orientation at some instant during progressive shearing. Such steady orientation of the mica fish in mylonites arises due to strain localization around the former as well as matrix anisotropy and reduced coherence at the object-matrix boundaries (ten Grotenhuis 2000). The presence of thin mantles of recrystallization around mineral fish (Fig. 3a) may reduce the coherence (as per Ceriani et al. 2003). The single sigmoid mineral fish studied from the KMC, on the other hand, demonstrated a wider range of local orientation covering lower values ($\alpha = 0\text{--}43^\circ$). Therefore, compared to the shear zones studied by ten Grotenhuis (2000) and Ceriani et al. (2003), the single mineral fish in the KMC seem to have undergone a more intensive ductile shearing. These mineral fish did not attain a stable orientation and therefore covers the lower limit of ' α ' values.

Tails of mica fish have been attributed to dynamic recrystallization along their tips (Lister and Snoke 1984). Simple shear-induced continuous pulling of the tips along the C-planes in opposite directions was considered as an alternate mechanism for the genesis of fish tails (Mawer 1987). If affected by secondary shearing, the tails show 'step-outs' or 'stair-steppings' (Lister and Snoke 1984).

Previous concepts of the genesis of single fish of micas and other minerals are of three broad types. (1) Simple shearing along with pressure solution: the combined process has been proposed to smooth the boundaries of a deforming mineral (Bell and Cuff 1989) leading to what has been defined in this work as the crest- and the trough regions (Fig. 4a) thereby giving rise to sigmoid fish (such as Fig. 3a–c; grains 1, 2 and 3 in Fig. 6a). (2) Simple shearing without any pressure solution: on rectangular micas. Such a process has been speculated to give parallelogram mica fish (Davis and Reynolds 1996; here Figs. 7, 8a, b, d, also c for garnet). Genesis of leucoxene fish has also been attributed to simple shear of pre-existing passive aggregates of leucoxenes (Oliver and Goodge 1996). An alternative qualitative explanation of the sigmoidality of the mica fish (such as Fig. 3a–c; grains 1, 2 and 3 in Fig. 6a) could be that the deforming mica grains cannot rotate in a direction perpendicular to the shear plane (Wilson 1984). The previous two types of concepts consider homogeneous simple shearing parallel to the C-planes. (3) Heterogeneous strain: such a strain on rectangular mineral grains can give

rise to shapes other than a parallelogram depending on the viscosity contrast between the clast and the surrounding matrix (Treagus et al. 1996; Treagus 2002; Treagus and Lan 2003). The model invokes neither the pressure solution of Bell and Cuff (1989) nor the rotational constraint of Wilson (1984). Using two-dimensional finite element analyses of pure shear deformation on incompetent rhomb-, square- and especially skew square-shaped inclusions within an incompressible fluid undergoing a quasi static type flow, Treagus and Lan (2000) obtained 'irregular hooked parallelogram' or 'string bean'-shaped clasts that are remarkably similar to the steep sigmoid or elongated sigmoid mineral fish. This finding is important since it also brackets the results for other inclusion shapes (Treagus 2002). Applying simple shear to ductile square objects in a matrix with low viscosity contrast much less than unity (viscosity ratio of clast to matrix = 0.1–0.001), Treagus and Lan (2004) simulated single sigmoid mineral fish that also depicted progressive changes in curvature at their corners.

This means, theoretically, starting from square inclusions and a certain inclusion-matrix viscosity contrast, both pure shear and simple shear can generate steep sigmoid and elongated sigmoid mineral fish. However, in reality, pure shear deformation on randomly oriented minerals would result in mineral fish that would not be indicative of any shear sense, and therefore they are expected to be variably oriented with their tangents at crests and troughs lacking any preferred orientation. None of the studied thin sections contained haphazardly oriented fish. Instead, the consistent top-to-SE sense of shear indicated by the mineral fish in the KMC (Figs. 3a–d, 4a–d; 8a–d, 10b, d, 12a–d) matches with the other shear sense indicators. This may indicate that the extreme rheological contrast between the clast and the matrix of the deformed rocks as in Treagus and Lan's (2000) model do not apply to the KMC rocks. Alternately, and perhaps plausibly, the top-to-SE simple shear was more intense than pure shear, if any, over individual mineral grains.

As mineral fish are defined morphologically and identified in different minerals, a single deformational process does not satisfactorily explain the genesis of all the subtypes of mineral fish. For example, individual cleaved blocks of single parallelogram mica fish undergo intra-granular slip along the (001) cleavage planes (grain '1' of Figs. 3d, 8a, b, d). A similar role of the (001) cleavage plane might be extrapolated in shaping the fish of other minerals consisting of one set of cleavage e.g., graphite (van der Pluijm 1991). However, for those minerals lacking cleavages such as garnet (Fig. 8c), crystal-plastic deformation of the mineral is the only obvious mechanism for producing the fish shape. Unlike the rotated porphyroblasts such as sigma- and delta-structures (e.g., Passchier and

Trouw 2005), the mineral fish does not appear to undergo significant rigid body rotation. Furthermore, two different processes may generate the same fish shape e.g., the parallelogram fish formed by primary shearing (grain '1' in Figs. 3d, 8a–d) looks similar to that formed by fracturing of an originally single sigmoid fish (grain '1' in Fig. 12d). During progressive simple shearing, steep sigmoid fish can be speculated to become elongated sigmoid fish with decreasing local orientation (α) and increasing aspect ratio (R) (cf. Hippertt 1994). Snake fish encountered in the KMC are always confined within secondary shear C' -planes. Hence, they have their origin in warping induced by secondary shearing (C') and exemplify the S - C' fabrics (Fig. 6b). Experimental/numerical investigation into composite mineral fish has been scanty. For example, simple shear deformation of homogeneously deformable polycrystalline aggregates with dislocation glide(s) as the dominant deformation mechanism (Etchecopar 1977) led to end products similar to parallelogram foliation fish (as Fig. 10d). Some of the cross-cutting mineral fish might have their origins in grain duplex movement where one grain overrides the other by cutting and thrusting in a piggy-back manner (Fig. 12a). Similar observation of grain duplex movement was made by Bowler (1987) at microscopic scales and by Bhattacharyya and Hudleston (2001) at mesoscopic scales from other shear zones. Internal mineral fish with both the host and the nucleated minerals having the same sense of ductile shearing (Fig. 12c) indicate either a pre-tectonic or a syn-tectonic nucleation. Here, 'tectonic' stands for the top-to-SE sense of ductile shearing in the KMC. Had the nucleation of the smaller mineral been post-tectonic, it could not have attained the sheared fish shape.

The present classification of mineral fish (Fig. 13), brief definition, alternate names used by other authors, their morphologies, geometric constrains (where specified) and deformation mechanism are summarized as follows.

(1) Single fish: Mineral fish defined by isolated minerals. $\alpha=0$ – 46° ; R : 1.35–11.1.

(1a) Sigmoid fish: Sigmoid-shaped fish. α : 0– 43° ; R : 2–11.1.

(1a1) Steep sigmoid fish: Sigmoid fish with α : 23– 43° ; R : 2.08–5.6. Similar to 'group-2 mica fish' of ten Grotenhuis et al. (2003); ' σ -Type porphyroclast system' of Simpson (1986); ' σ_a -Type porphyroclast system' of Passchier and Simpson (1986); 'porphyroclastic type' of Blenkinsop and Treloar (1995). Genesis: simple shearing and pressure solution at corners.

(1a2) Elongated sigmoid fish: Sigmoid fish with α : 7– 23° ; R : 3.1–10. Similar to 'banded type porphyroclasts' of Blenkinsop and Treloar (1995). Genesis: extensive simple shearing and pressure solution at corners.

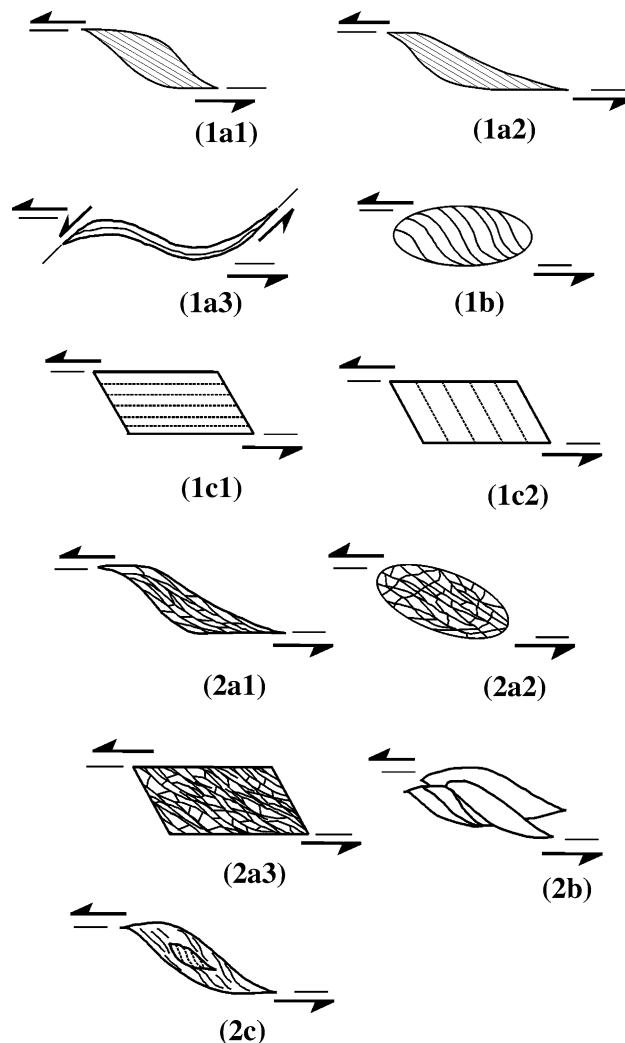


Fig. 13 Morphological types of mineral fish: (1) single fish; (1a) sigmoid fish; (1a1) steep sigmoid fish; (1a2) elongated sigmoid fish; (1a3) snake fish; (1b) lenticular fish; (1c) parallelogram fish; (1c1) l-parallelogram fish; (1c2) r-parallelogram fish; (2) composite fish; (2a) foliation fish; (2a1) sigmoid foliation fish; (2a2) lenticular foliation fish; (2a3) parallelogram foliation fish; (2b) cross-cutting fish; (2c) internal fish

(1a3) Snake fish: Sigmoid fish with α : 0– 7° ; R : 2.6–11.1. Similar to group-6 mica fish of ten Grotenhuis et al. (2003). Genesis: secondary synthetic shearing leading to lowering of ' α '.

(1b) Lenticular fish: Elliptical. α : 0– 35° ; R : 1.35–6.2. Similar to 'augens' in augen-gneisses; 'group-1 and -5 mica fish' of ten Grotenhuis et al. (2003).

(1c) Parallelogram fish: Parallelogram shaped. α : 30– 46° ; R : 3.13–6.8. Genesis: simple shearing without pressure solution at corners.

(1c1) l-parallelogram fish: Similar to group-3 mica fish of ten Grotenhuis et al. (2003).

(1c2) r-parallelogram fish: Similar to group-4 mica fish of ten Grotenhuis et al. (2003).

(2) Composite fish: Mineral fish defined by an aggregate of minerals.

(2a) Foliation fish: Ductile sheared aggregates of minerals. Similar to ‘foliation fish’ of Dennis and Secor (1987), Hammer and Passchier (1991), Davis and Reynolds (1996), Stephenson (1997), Lin (1999), Stephenson et al. (2000), Passchier and Trouw (2005) and Trouw et al. (2010).

(2a1) Sigmoid foliation fish: Sigmoid-shaped foliation fish.

(2a2) Lenticular foliation fish: Lenticular-shaped foliation fish.

(2a3) Parallelogram foliation fish: Parallelogram-shaped foliation fish.

(2b) Cross-cutting fish: One mineral fish partially or completely cuts across the other, may indicate thrust movement of one grain over the other.

(2c) Internal fish: One mineral fish nucleates inside the other mineral fish. Pre- or syn-tectonic nucleation of the smaller fish inside the host fish.

Conclusions

- Mineral fish are generally asymmetric-shaped mineral grains in sheared rocks. Oriented thin sections of sheared rocks of the Karakoram Metamorphic Complex reveal a total of 11 sub-types of mineral fish consistently showing a top-to-SE sense of ductile shearing. Nine of these sub-types are defined by three broad geometries- sigmoid, lenticular and parallelogram that incorporate either single or an aggregate of minerals. One mineral fish cut by another defines cross-cutting fish and the nucleation of one mineral fish within another defines internal fish. Single sigmoid mineral fish vary widely in their local orientations and aspect ratios with the presence of natural breaks in the magnitude of the former parameter. Two of the boundaries of the internal fish parallel the cleavages of the host mineral fish. Their wide range of local orientations including low values implies that the mineral fish in the study area underwent extensive ductile shearing. Fish tails are the products of stretching of the fish tips along with dynamic recrystallization.
- The asymmetry and inclination of all the fish sub-types to the C-planes reliably indicate a top-to-SE sense of ductile shearing. In different single fish, the cleavage planes show variation in curvature. Very rarely, cleavages of fish are antithetically oriented to the shear direction rendering the former as unreliable shear sense indicators. Parallelogram-shaped mineral grains observed on a randomly grown mineral aggregates are discriminated

from mineral fish and are not shear sense indicators. Orientations of the individual minerals in composite fish are not indicative of any shear sense.

- Mineral fish can be produced by simple shearing in a homogeneous deformation with or without pressure solution. Heterogeneous deformation or pure shear leading to their genesis is implausible since mineral fish in the study area are not haphazard in orientation. Some varieties of mineral fish could also have formed by intra-granular slip along cleavage planes or by crystal-plastic deformation of the whole grain. Late fracturing can generate a new fish from another. Prolonged synthetic shearing on minerals can lead to snake fish. Simple shear on mineral aggregates can result in parallelogram foliation fish. Some of the cross-cutting fish may indicate duplex movements amongst mineral grains. The internal fish nucleated either prior to or during the top-to-SE sense of shearing.

Acknowledgments Indian Institute of Technology Bombay’s *Seed Grant: Spons/GS/SM-1/2009* supported this work. Geology students (2002–2007) at IIT Roorkee taught me microstructures when I was their Teaching Assistant. Ramananda Chakrabarti (Harvard University), Sidhartha Bhattacharyya (Alabama University), Arundhuti Ghatak (Rochester University) and Pritam Nasipuri (Universitetet i Tromsø) constantly updated me on microstructures. Emeritus Professor Christopher J. Talbot (Uppsala University) is heartily thanked for going through different versions of the script as an ‘internal reviewer’, for his geologic and linguistic inputs and for suggesting a more appropriate term ‘internal fish’ in place of ‘swallowed fish’. Mary Leech (San Francisco State University) and Richard Norris (University of Otago) are gratefully acknowledged for insightful reviews, which led to significantly fine tune the manuscript. Richard’s comments prompted me to revise the mineral fish classification presented here and be extremely cautious in using parallelogram-shaped grains as shear sense indicators. Teaching Assistant Nayani Das (IIT Bombay) reformatted some of the line diagrams. Springer team’s intense proof-reading is appreciated.

References

- Bell TH (1981) Foliation development-the contribution, geometry and significance of progressive, bulk, inhomogeneous shortening. *Tectonophysics* 75:273–296
- Bell TH, Cuff C (1989) Dissolution, solution transfer, diffusion versus fluid flow and volume loss during deformation/metamorphism. *J Meta Geol* 7:425–447
- Bhattacharyya P, Hudleston P (2001) Strain in ductile shear zones in the Caledonides of northern Sweden: a three-dimensional puzzle. *J Struct Geol* 23:1549–1565
- Blenkinsop TG, Treloar PJ (1995) Geometry, classification and kinematics of S-C and S-C’ fabrics in the Mushandike area, Zimbabwe. *J Struct Geol* 17:397–408
- Bowler S (1987) Duplex geometry: an example from the Moine Thrust Belt. *Tectonophysics* 135:25–35
- Ceriani S, Mancktelow NS, Pennacchioni G (2003) Analogue modeling of the influence of shape and particle/matrix interface lubrication on the rotational behaviour of rigid particles in simple shear. *J Struct Geol* 25:2005–2021

- Davis GH, Reynolds SJ (1996) Structural geology of rocks and regions, 2nd edn. Wiley, New York, p 547
- Dennis AJ, Secor DT (1987) A model for the development of crenulations in shear zones with applications from the Southern Appalachian Piedmont. *J Struct Geol* 9:809–817
- Eisbacher GH (1970) Deformation mechanisms of mylonitic rocks and fractured granulites in Cobequid Mountains, Nova Scotia Canada. *Geol Soc Am Bull* 81:2009–2020
- Etchecopar A (1977) A plane kinematic model of progressive deformation in a polycrystalline aggregate. *Tectonophysics* 39:121–139
- Godin L, Grujic D, Law RD et al (2006) Channel flow, extrusion and extrusion in continental collision zones: an introduction. In: Law RD, Searle MP (eds) Channel flow, extrusion and extrusion in continental collision zones, vol 268. Geological Society London Special Publication, pp 1–23
- Hanmer S, Passchier C (1991) Shear-sense indicators: a review. Geological Survey of Canada Paper 90-17, 72 p
- Hippertt JF (1994) Microstructure and c-axis fabrics indicative of quartz dissolution in sheared quartzites and phyllonites. *Tectonophysics* 229:141–163
- Jain AK, Singh S (2008) Tectonics of the southern Asian Plate margin along the Karakoram Shear Zone: constraints from field observations and U-Pb SHRIMP ages. *Tectonophysics* 451:186–205
- Jain AK, Singh S, Manickavasagam RM et al (2003) HIMPROBE programme: integrated studies on geology, petrology, geochronology and geophysics of the Trans Himalaya and Karakoram. Memoir Geological Society of India No. 53
- Kula J, Tulloch A, Spell TL et al (2007) Two-stage rifting of Zealandia-Australia-Antarctica: Evidence from $^{40}\text{Ar}/^{39}\text{Ar}$ thermochronometry of the Sisters shear zone, Stewart Island, New Zealand. *Geology* 35:411–414
- Lin A (1999) S-C cataclasis in granitic rocks. *Tectonophysics* 304:257–273
- Lister GS, Snoke AW (1984) S-C Mylonites. *J Struct Geol* 6:617–638
- Little TA, Holcombe RJ, Ilg BR (2002) Ductile fabrics in the zone of active oblique convergence near the Alpine Fault, New Zealand: identifying the neotectonic overprint. *J Struct Geol* 24:193–217
- Mancktelow NS, Arbaret L, Pennacchioni G (2002) Experimental observations on the effect of interface slip on rotation and stabilization of rigid particles in simple shear and a comparison with natural mylonites. *J Struct Geol* 24:567–585
- Mawer CK (1987) Shear criteria in the Grenville Province, Ontario, Canada. *J Struct Geol* 9:531–539
- Mukherjee S (2007) Geodynamics, deformation and mathematical analysis of metamorphic belts of the NW Himalaya. Unpublished Ph.D. thesis. Indian Institute of Technology Roorkee, pp 1–267
- Mukherjee S (2010a) Structures at meso and micro-scales in the Sutlej section of the higher Himalayan shear zone in Himalaya. *e-Terra* 7(1):1–27. <http://metododirecto.pt/ojs/index.php/e-terra/article/view/33/21>
- Mukherjee S (2010b) Microstructures of the Zaskar Shear Zone. *Earth Sci India* 3(1):9–27. <http://www.earthscienceindia.info/PDF/Mukerjee.pdf>
- Mukherjee S, Koyi HA (2010a) Higher Himalayan Shear Zone, Sutlej Section—structural geology & extrusion mechanism by various combinations of simple shear, pure shear & channel flow in shifting modes. *Int J Earth Sci* (in press)
- Mukherjee S, Koyi HA (2010b) Higher Himalayan Shear Zone, Zaskar Section- microstructural studies & extrusion mechanism by a combination of simple shear & channel flow. *Int J Earth Sci* (in press)
- Mukherjee S, Pal P (2000) Tectonic structures of the Karakoram metamorphic belt, its significance in the geodynamic evolution. Unpublished Report. Summer Undergraduate Research Award. University of Roorkee
- Oliver DH, Goodge JW (1996) Leucoxene fish as a micro-kinematic indicator. *J Struct Geol* 18:1493–1497
- Passchier CW, Simpson C (1986) Porphyroclast systems as kinematic indicators. *J Struct Geol* 8:831–843
- Passchier CW, Trouw RAJ (2005) *Microtectonics*. Springer, Heidelberg
- Simpson C (1986) Fabric development in brittle-to-ductile shear zones. *Pure Appl Geophys* 124:269–288
- Simpson C, Schmid SM (1983) An evaluation of criteria to deduce the sense of movement in sheared rocks. *Bull Geol Soc Am* 94:1281–1288
- Singh K (2003) Microstructural changes in quartzite across the MCT zone, Western Garhwal Himalaya. *Himal Geol* 24:91–99
- Stephenson BJ (1997) The tectonic and metamorphic evolution of the Main Central Thrust zone and High Himalaya around the Kishtwar and Kulu windows, Northwest India. D.Phil thesis. Oxford University, Oxford
- Stephenson BJ, Waters DJ, Searle MP (2000) Inverted metamorphism and the Main Central Thrust: field relations and thermobarometric constraints from the Kistwar Window, NW Indian Himalaya. *J Meta Geol* 18:571–590
- ten Grotenhuis SM (2000) Mica fish in mylonites. Ph.D thesis (unpublished). Johannes Gutenberg Universität Mainz, Germany. <http://ArchiMeD.uni-mainz.de/pub/2001/0033/diss.pdf>
- ten Grotenhuis SM, Passchier CW, Bons PD (2002) The influence of strain localization on the rotation behaviour of rigid objects in experimental shear zones. *J Struct Geol* 24:485–499
- ten Grotenhuis SM, Trouw RAJ, Passchier CW (2003) Evolution of mica fish in mylonitic rocks. *Tectonophysics* 372:1–21
- Thakur VC (1992) *Geology of western Himalaya*. Pergamon Press, Oxford
- Treagus SH (2002) Modelling the bulk viscosity of two-phase mixtures in terms of clast shape. *J Struct Geol* 24:57–76
- Treagus SH, Lan L (2000) Pure shear deformation of square objects, and applications to geological strain analysis. *J Struct Geol* 22:105–122
- Treagus SH, Lan L (2003) Simple shear of deformable square objects. *J Struct Geol* 25:1993–2003
- Treagus SH, Lan L (2004) Deformation of square objects and boudins. *J Struct Geol* 26:1361–1376
- Treagus SH, Hudleston PJ, Lan L (1996) Non-ellipsoidal inclusions as geological strain markers and competence indicators. *J Struct Geol* 18:1167–1172
- Trouw RAJ, Passchier CW, Wiersma DJ (2010) *Atlas of Mylonites and related microstructures*. Springer, Heidelberg, pp 189
- van der Pluijm BA (1991) Marble mylonites in the Bancroft shear zone, Ontario, Canada: microstructures and deformation mechanisms. *J Struct Geol* 13:1125–1136
- Wilson CJL (1984) Shear bands, crenulations and differentiated layering in ice-mica models. *J Struct Geol* 6:303–320
- Zhu G, Liu GS, Niu ML et al (2007) Syn-collisional transform faulting of the Tan-Lu fault zone, East China. *Int J Earth Sci* 98:135–155